WCTE 2016
World Conference on Timber Engineering
August 22-25, 2016 | Vienna, Austria

2D NON-PRISMATIC BEAM MODEL FOR STIFFNESS MATRIX EVALUATION

Valentina Mercuri[1], Giuseppe Balduzzi[2], Domenico Asprone[3], Ferdinando Auricchio[4]

ABSTRACT: Variable coefficients and complex relations generally characterize the differential equations governing non-prismatic beam behaviour. This leads to employ either complex and expensive analysis or simplified (and often inaccurate) approaches. This work aims at illustrating a 2D model for the study of beams with variable cross-section, model which is accurate but, at the same time, practical enough to be used in engineering applications. Based on the Hellinger-Reissner functional and a dimensional reduction approach, the developed theory exploits the familiar Timoshenko-kinematic, while the variables assumed for the stress definition are directly correlated to the general forces. Thus, once the stresses are calculated, the Finite Element (FE) stiffness matrix is easily recovered. The efficiency of the model is tested through some examples and resulting stiffness coefficients are compared to those obtained with an accurate 2D analysis. Final considerations and results confirm the efficiency of the method.

KEYWORDS: non-prismatic members, beam model, stiffness matrix, numerical analysis

1 INTRODUCTION

Non-prismatic members are commonly used to optimize the amount of material and strength, achieve a better distribution of the internal stresses, reduce the dead load, and sometimes to satisfy architectural and functional requirements in many engineering structures such as bridges, roof, space and aircraft structures. Particularly in the field of timber buildings, glued laminated beams are often tapered for drainage, appearance, to provide pitched roofs, and to save weight. Some sensitive aspects have to be considered in the modelling of such particular elements. Many standard engineering methods analyse beams of uniform and variable depth based on Bernoulli-Euler or Timoshenko beam theories, which are adequate as long as the tapering remains negligible [1]. Furthermore, in non-prismatic beams the locus of cross-section centroids does not coincide with the beam axis, producing a strong coupling between the bending moment, shear, and axial forces [2]. Another aspect that is often overlooked is the equilibrium on the beam lateral surface, which reveals that non-vanishing shear stresses exist at top and bottom fibres of the beam [3,4]. Unfortunately, several methods in available literature adopt approximations that lead to neglect one or more of the aforementioned aspects. Another bad practice is the straightforward early technique of dividing a tapered beam into a number of uniform elements, which has been shown lowly efficient and accurate [3].

1.1 LITTERATURE REVIEW

As introduced in the abstract, in this study we want to focus on FE stiffness matrix evaluation, which is a key point in structural analysis. Within a large body of papers on the stiffness formulation for non-prismatic beams, one of the first contributions was provided by Just [5] with a formulation based on the Euler-Bernoulli theory. The stiffness terms were expressed as a function of basic flexibility terms, computed by evaluating their corresponding integrals. Later, Browns [6] presented a method where approximate interpolation functions were used to obtain bending stiffness matrix. Starting from flexibility method, Eisenberger [7] derived matrix coefficients for members with variable cross-section, taking into account height and width variation; while Tena-Colunga [8] included shear deformation and the variability of the cross-section in order to be effective

[1]Valentina Mercuri, Università degli Studi di Pavia, Department of Civil Engineering and Architecture, via Ferrata 3, 27100, Pavia, valentina.mercuri01@universitadipavia.it
[2] Giuseppe Balduzzi, IMWS Vienna University of Technology, Giuseppe.Balduzzi@tuwien.ac.at
[3] Domenico Asprone, Università degli Studi di Napoli "Federico II", domenico.asprone@unina.it
[4] Ferdinando Auricchio, Università degli Studi di Pavia, ferdinando.auricchio@unipv.it

both for 2D and for 3D tapered members. Unfortunately, all these researches suffer the common weaknesses of neglecting the aforementioned boundary equilibrium and coupling effect occurring in tapered elements.
As technology and computer science were developing, numerical analysis has become very popular in several engineering fields, resulting particularly useful in problems described by complex differential equations. For this reason, such techniques started to be frequently used for the study of beams with variable cross-section and for the derivation and implementation of the FE stiffness matrix. Among the recent papers, a two-node beam element having average inertia and area was proposed by Balkaya [9] after the study of the behavior of haunched beam having T-section using 3D FE models. Zhi-Luo et al. [10] exploited the Transfer Matrix Method (TMM) for continuous and discontinuous non-prismatic members. Gimena et al. [11, 12] studied spatial arch problems exploiting the finite transfer method and the stiffness matrices method. They provide both analytic exact and numerical approximate procedures for widely spread cases of curved beams, considering different support conditions in order to obtain accurate results. Unfortunately, the most of them do not tackle adequately the effects induced by boundary equilibrium, resulting therefore inaccurate for practical uses. The procedure proposed by Shooshtari et al. [13] investigated shape functions and stiffness matrices of non-prismatic beams and it was based on considering rigid body motions separated from other strain states. These are only a limited number of the investigations carried out on the topic. Despite the research effort of the last decades, there is still the need of an efficient approach in numerical methods involving non-uniform and discontinuous beam. In fact, some of these methods started from conventional formulations recovering the stiffness matrix only for some special simple geometries, for others it is not possible to retrieve shape functions, which might be necessary for the analysis based on stiffness formulations. Furthermore, the complexity and accuracy of the predictive model has to be balanced with analysis computational costs and time consumption.

With the proposed model, we want to overcome these issues, providing a functional tool particularly useful for the evaluation of the elastic stiffness matrix of non-prismatic beams. The model comes from the generalization of a procedure illustrated by Auricchio et al. [14], and later developed by Beltempo et al. [15]. The approach adopted for the derivation is the so-called dimensional reduction method, starting from the Hellinger-Reissner (HR) functional.
The document is structured as follows: Section 2 summarizes the assumptions considered for the model, deepening some aspects related to variable selection and the derivation of the FE stiffness matrix; Section 3 contains results from numerical tests made on different geometry in order to verify and validate the model; in Section 4 final considerations about the output and the extensions of the theory are discussed.

2 2D NON-PRISMATIC MODEL

In this section some specific aspects of the proposed model are recalled, in order to clarify equations and parameters adopted in the paper. Particularly, we focus on the hypotheses on stress and displacement fields and on the evaluation of the problem unknowns. For a detailed description of the beam model, readers may refer to [15].

2.1 GEOMETRY DEFINITION

The object of the study is a generic planar and homogeneous body Ω, considering a case in which the plane-stress-state hypothesis can be imposed to a 3D body since its width is negligible. Such body behaves under the assumptions of small displacements and linear elastic isotropic constitutive law. The reference system is suitably chosen, with the x axis straight and normal to the cross-section axis y. In order to define the domain Ω, two sufficiently smooth functions $h_u(x)$ and $h_l(x)$ (such that $h_l(x) < h_u(x) \ \forall \ x \in l$) are introduced to describe the geometry of the upper and lower bounds of the domain respectively. $A(0)$ and $A(L)$ are the cross-section area at $x = 0$ and $x = L$. The function $c(x)$ defines the y coordinates of the cross-section centroids, while $t(x)$ is the cross-section depth assumed as a positive definite function. Therefore, $h_u(x)$ and $h_l(x)$ can be expressed as functions of $c(x)$ and $t(x)$ as follow:

$$h_u(x) = c(x) + \frac{t(x)}{2} \tag{1a}$$

$$h_l(x) = c(x) - \frac{t(x)}{2} \tag{1b}$$

Figure 1 summarizes the information described above and used in model formulation.

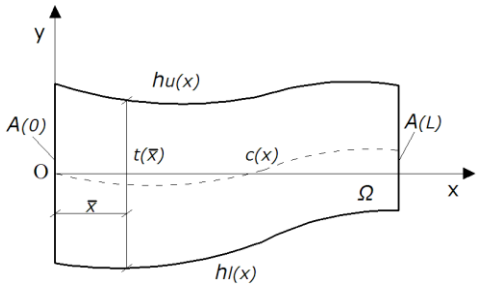

Figure 1: *Generic non-prismatic beam*

2.2 MODEL FORMULATION

Recalling as extensively discussed by Beltempo et al. [15], the approach adopted for the beam model derivation is the so-called dimensional reduction method, starting from the Hellinger-Reissner (HR) functional in which displacement $\boldsymbol{s}$ and stress $\boldsymbol{\sigma}$ are the unknown fields [14, 15]. Introducing appropriate hypotheses on stress and displacement fields, the dimensional reduction allows reducing the integral over

a 2D domain, associated with the HR functional, into an integral over a 1D domain. This is also possible thanks to the exploitation of the domain structure.

The general system of ordinary differential equations for the 1D problem is written as follow:

$$\begin{cases} G\begin{Bmatrix} s' \\ \sigma' \end{Bmatrix} + H\begin{Bmatrix} s \\ \sigma \end{Bmatrix} = \begin{Bmatrix} F \\ 0 \end{Bmatrix} & \text{in } l \\ + \quad BCs \end{cases} \tag{2}$$

where G and H are matrices of non-constant coefficients governing the HR model, and F is the beam distributed load. Considering the scalar components of $\boldsymbol{s}$ and $\boldsymbol{\sigma}$, for the displacement field the authors maintained the simple Timoshenko kinematics, assuming the horizontal $s_u(x,y)$ and the vertical $s_v(x,y)$ respectively as a linear and a constant function of y :

$$s_u(\mathrm{x},\mathrm{y}) = u_0(x) + \tilde{y}\frac{t(x)}{2}\theta(x) \tag{3a}$$

$$s_v(\mathrm{x},\mathrm{y}) = v_0(x) \tag{3b}$$

For the stress field they assumed $\sigma_{xx}(x,y)$ and $\sigma_{yy}(x,y)$ linear respect to y, while $\sigma_{xy}(x,y)$ is a quadratic function of y. These hypotheses on the $\boldsymbol{\sigma}$ field together with the boundary equilibrium conditions on the edge surfaces lead to the following expressions:

$$\sigma_{xx}(\mathrm{x},\mathrm{y}) = \sigma_{x0}(x) + \tilde{y}\sigma_{x1}(x) \tag{4a}$$

$$\sigma_{yy}(\mathrm{x},\mathrm{y}) = \left(c'^2(x) + \frac{1}{4}t'^2(x)\right)\left(\sigma_{x0}(x)\tilde{y} + \sigma_{x1}(x)\right) + t'(x)c'(x)\left(\sigma_{x1}(x)\tilde{y} - \sigma_{x0}(x)\right) \tag{4b}$$

$$\sigma_{xy}(\mathrm{x},\mathrm{y}) = \left(c'(x)\sigma_{x0}(x) - \frac{t'(x)}{2}\sigma_{x1}(x)\right) + \left(\frac{t'(x)}{2}\sigma_{x0}(x) - c'(x)\sigma_{x1}(x)\right)\tilde{y} + \frac{3}{2}\tau(x)(1-\tilde{y}^2) \tag{4c}$$

where the linear function $\tilde{y}$ is introduced for convenience of representation, it is defined as in (5) and it is equal to 1 at $h_u(x)$, 0 at $c(x)$ and -1 at $h_l(x)$:

$$\tilde{y} = \left(c(x) - y\right)\frac{2}{t(x)} \tag{5}$$

For the illustrated hypotheses $u_0(x)$, $v_0(x)$, $\theta(x)$ are the displacement independent variables , while $\sigma_{x0}(x)$, $\sigma_{x1}(x)$, $\tau(x)$ are the stress independent variables.

Even though the form of the stress distributions does not represent a difficulty for the system resolution, we introduce some modifications to the expressions (4c) in order to further simplify the use of the model. In the following equations we use the notation used in [15]:

$$G = \begin{bmatrix} 0 & -G_{s\sigma} \\ G_{s\sigma} & 0 \end{bmatrix} \tag{6}$$

$$G_{s\sigma} = \int_A R_s^T E_1 R_\sigma dy \tag{7}$$

$$\sigma = \begin{Bmatrix} \sigma_{x0}(x) \\ \sigma_{x1}(x) \\ \tau(x) \end{Bmatrix} \tag{8}$$

where R_s and R_σ are matrices of coefficients obtained switching respectively the displacement (3a-b) and the stress (4a-c) hypotheses into the engineering notation, and E_1 is a Boolean matrix. Handling with the matrix G used in (2), from the product of $G_{s\sigma}$ with the vector it is possible to recover the relationship between stress independent variables and the generalized stresses:

$$\begin{Bmatrix} \sigma_{x0}(x)t(x)b \\ \sigma_{x1}(x)\frac{t^2(x)}{6}b \\ t(x)(c'(x)\sigma_{x0}(x) - \tau(x)) - \frac{t(x)}{2}t'(x)\sigma_{x1}(x) \end{Bmatrix} = \begin{Bmatrix} N(x) \\ M(x) \\ -V(x) \end{Bmatrix} \tag{9}$$

from the last of the system we obtain:

$$\tau(x) = -\frac{V(x)}{t(x)} - c'(x)\sigma_{x0}(x) + \frac{t(x)}{2}t'(x)\sigma_{x1}(x) \tag{10}$$

The integral of the variable $\tau(x)$ over $A(x)$ does not correspond to the shear force $V(x)$. In order to recover $V(x)$ from the conventional relations known for prismatic beam, we substitute $\tau(x)$ of (4c) with expression (10) and after properly reassembling we obtain:

$$\sigma_{xy}(\mathrm{x},\mathrm{y}) = \left(c'(x)\sigma_{x0}(x) - \frac{t'(x)}{2}\sigma_{x1}(x)\right)\left(-\frac{1}{2} + \frac{3}{2}\tilde{y}^2\right) + \left(c'(x)\sigma_{x1}(x) - \frac{t'(x)}{2}\sigma_{x0}(x)\right)\tilde{y} + \frac{3}{2}\tilde{\tau}(x)(1-\tilde{y}^2) \tag{11}$$

The new introduced variable $\tilde{\tau}(x)$ is directly correlated to the shear force $V(x)$, as $\sigma_{x0}(x)$ and $\sigma_{x1}(x)$ to $N(x)$ and $M(x)$. In fact, using expression (11) instead of (4c) with the hypotheses (4a-b), system (9) becomes:

$$\begin{Bmatrix} N(x) \\ M(x) \\ -V(x) \end{Bmatrix} = \begin{Bmatrix} \sigma_{x0}(x)t(x)b \\ \sigma_{x1}(x)\frac{t^2(x)}{6}b \\ \tilde{\tau}(x)t(x)b \end{Bmatrix} \tag{12}$$

Using hypotheses indicated for $\boldsymbol{s}$ (expressions (3a-b)) and particularly for $\boldsymbol{\sigma}$ field (expressions (4a-c)) together with relations in (12), the beam model can be expressed as a set of explicit ODEs, as follows:

$$\begin{Bmatrix} N'(x) \\ M'(x) \\ V'(x) \\ u_0'(x) \\ \theta_0'(x) \\ v_0'(x) \end{Bmatrix} = \begin{Bmatrix} H_{1,1} & . & . & H_{1,6} \\ . & . & & \\ . & & . & \\ H_{6,1} & & & H_{6,6} \end{Bmatrix} \begin{Bmatrix} N(x) \\ M(x) \\ V(x) \\ u_0(x) \\ \theta_0(x) \\ v_0(x) \end{Bmatrix} - \begin{Bmatrix} f_x(x) \\ m(x) \\ f_y(x) \\ 0 \\ 0 \\ 0 \end{Bmatrix} \quad (13)$$

where $H_{i,j}$ are the components of the coefficient matrix, while $f_x(x)$, $m(x)$ and $f_y(x)$ represent respectively the horizontal, the vertical and the bending components of the distributed load vector. In the resulting system of ODEs, shear component is recovered through the new stress independent variable $\tilde{\tau}(x)$.

For simplicity of notation, in reporting the coefficients of the matrix we omit the dependence on the axial coordinate x after each variable (and coefficients not reported are zero components of the matrix).

$$H_{2,1} = c \quad (14a)$$

$$H_{2,3} = 1 \quad (14b)$$

$$H_{3,1} = \frac{-(2c' + t')^2}{2t} \quad (14c)$$

$$H_{3,2} = \frac{3(2c' + t')^2}{t^2} \quad (14d)$$

$$H_{4,1} = \frac{240 + 96(1+\nu)c'^2 + 80c'^4 + 480\nu c' t}{240bEt} + \frac{40\left(1 + \nu + 7c'^2\right)t'^2 + 5c'^4}{240bEt} \quad (14e)$$

$$H_{4,2} = -\frac{2\left[20\nu c'^2 + 20c'^3 t' + 5\nu t'^2 + c' t'\left(8 + 8\nu + 5t'^2\right)\right]}{5bEt^2} \quad (14f)$$

$$H_{4,3} = \frac{2(1+\nu c')^2}{5bEt} \quad (14g)$$

$$H_{5,1} = H_{4,2} \quad (14h)$$

$$H_{5,2} = \frac{240 + 720c'^4 + 480\nu c' t' + 72\left(1 + \nu t'^2\right)}{20bEt^3} + \frac{45t'^4 + 120c'^2\left(4 + 4\nu t'^2 + 5t'^2\right)}{20bEt^3} \quad (14i)$$

$$H_{5,3} = -\frac{6(1+\nu)t'}{5bEt^2} \quad (14l)$$

$$H_{6,1} = -H_{4,3} \quad (14m)$$

$$H_{6,2} = -H_{5,3} \quad (14n)$$

$$H_{6,3} = -\frac{12(1+\nu)}{5Ebt} \quad (14o)$$

$$H_{4,5} = -H_{2,1} \quad (14p)$$

$$H_{4,6} = H_{3,1} \quad (14q)$$

$$H_{5,6} = H_{3,2} \quad (14r)$$

$$H_{6,5} = H_{2,3} \quad (14s)$$

It is worth to notice that equations (12) formally recalls the conventional relations known for prismatic beams. The use of (12) also in the case of beams with variable cross-section is possible thanks to the introduction of the variable $\tilde{\tau}(x)$, which is differentiated on purpose from the other stress quantities whit the hat tilde. The shear stress component relation (11) is, in fact, obtained after appropriate manipulations on the $\sigma_{x,y}(x,y)$ hypotheses, which allow to decouple the V(x) from $\sigma_{x0}(x)$ and $\sigma_{x1}(x)$. However, as consequence of such manipulations, the respect of equilibrium conditions on the section surfaces is neglected leading to an inexact prediction of stress distribution over the section. Conversely, abiding by the boundary equilibrium naturally introduces non-trivial relations between all stress independent variables and V(x), leading to a different expression for the $\sigma_{x,y}(x,y)$ component in (4c) and consequently to a more complex relation for the third row of system (9).

This clarification is aimed at stressing that there is freedom in the choice of the hypotheses and they are related to the purpose of the problem. The aim of this work is individuate a simple and correct procedure for the derivation of the stiffness matrix of a generic non-prismatic beam. Stiffness matrix coefficients evaluated with the set of hypotheses presented above or considering the boundary equilibrium as in Beltempo [15] are the same in value. This is possible because in terms of resulting forces, the shape of the stress distribution does not affect the correctness of the results. The algebraic manipulations of equations (4c) are only made to simplify the use of the model and to make possible the use of the well-known relations (12). In fact, solving the ODEs system (13) it is possible to recover displacement unknowns and reactions forces directly from stress variables with (12), thus we compute the beam's characteristic forces and consequently the stiffness coefficients.

The modelling approach allows tackling any complex shear stress distribution directly in the 2D problem formulation, leading to the resulting relations automatically. In this work, we adopted an ad hoc set of hypotheses for the stress field because they make possible the use of the well-known prismatic relations also for non-prismatic beams without interfering in the calculus of stiffness matrix coefficients. Considering a different set of hypotheses, for example that used in [15], it is possible to recover the cross-section stress distribution thanks to the generality of the model. This could be particularly advantageous in the study of timber members, in which the correct evaluation of the forces, displacement and stress distribution is fundamental and variable shapes are very common.

3 NUMERICAL TESTS AND MODEL VERIFICATION

In the paper presented by Beltempo et al. [15] the principal aim was to test the model in predicting stresses and displacements considering different geometries, load cases and boundary conditions. Here, the purpose is to explore the potential of the method for the evaluation of the stiffness matrix of a generic non-prismatic beam element.

In order to test the model accuracy, the stiffness matrix K^{Mod} obtained for different geometries are compared with those calculated by the finite element software Abaqus [16] (K^{Ref}), considered as the 2D FE reference solution. Limiting the attention to linear elastic isotropic material, as test cases we consider both the non-symmetric and the symmetric tapered beam case. Among the studied geometries, we decide to deepen the parametric study for the non-symmetric tapered case because this specific geometry quite often recurs in structural system (as example in reinforced concrete moment frames [17] and double pitched glued laminated timber beams). For this case the matrix comparison is carried on also with results obtained from the Timoshenko theory equations (K^{T}), introducing variable geometric parameters (area and inertia modulus).
For the sake of completeness, we also report the symmetric tapered case. In fact, even if the symmetric case is more trivial respect to the non-symmetric one, it is a classic case study recurring in literature.

3.1 NON-SYMMETRIC TAPERED BEAM: PARAMETRIC STUDY

The first analysed geometry is a non-symmetric tapered beam in accordance with Figure 2.

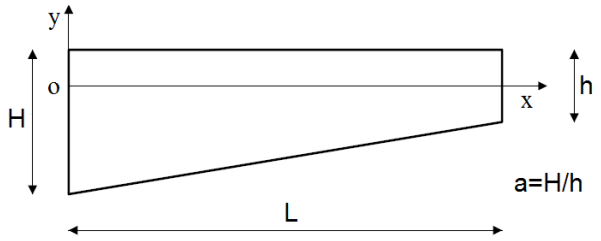

Figure 2: *Non-symmetric tapered beam geometry*

The parametric study consists in varying the parameter a (defined as the ratio between the maximum height H and the minimum height h from 1 to 8, and in considering the ratio $H/L_1 = 1/10$ (slender beam) and $H/L_2 = 1/5$ (squat beam). The angles between the lower edge of the beam and the horizontal axis are indicated with α , calculated respectively for $L_1 = 4m$ and $L_2 = 2m$. Table 1 summarizes characteristics of the 10 different cases considered. Moving from one case to another, the height H is kept constant and the variables are the lower height and the beam length**.** Considering different values of parameter a allows highlighting the influence of taper on results effectiveness. As illustrated in section 2, recovering stresses and matrix coefficients using the presented model is practically immediate once solved system (13). Obtained stiffness matrices are associated to the set of nodal degrees of freedom (DOFs) reported in Figure 3. Particularly, considering Figure, we assume that the matrix form and the vector of unknowns of stiffness equation is:

$$K \cdot \begin{Bmatrix} \hat{u}_1 \\ \hat{v}_1 \\ \hat{\theta}_1 \\ \hat{u}_2 \\ \hat{v}_2 \\ \hat{\theta}_2 \end{Bmatrix} = \begin{Bmatrix} N_1 \\ V_1 \\ M_1 \\ N_2 \\ V_2 \\ M_2 \end{Bmatrix} \tag{15}$$

Table 1: *Summary of studied cases for the stiffness matrix evaluation of the non-symmetric tapered case*

L [m]	H [m]	h [m]	a [-]	α [°]
4	0.4	0.4	1	0
4	0.4	0.2	2	2.9
4	0.4	0.1	4	4.3
4	0.4	0.0666	6	4.8
4	0.4	0.05	8	5
2	0.4	0.4	1	0
2	0.4	0.2	2	5.7
2	0.4	0.1	4	8.5
2	0.4	0.0666	6	9.5
2	0.4	0.05	8	10

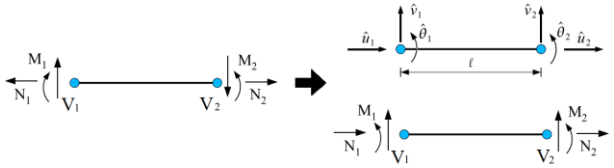

Figure 3: *Set of nodal DOFs and sign convention*

Concerning Abaqus analysis, we implemented the 2D FE models adopting a 4-node bilinear plane-stress quadrilateral element. The mesh is characterized by an approximate element size of 0.003 m. This particular choice comes from an accurate mesh-convergence, according to the number of digits used in reporting numerical results.

3.1.1 Considerations on Timoshenko's model

As shown in the following matrices related to the slender beam case $(H/L_1 = 1/10)$ for a taper ratio $a = 2$, Timoshenko equations are no longer usable when the section change from prismatic to tapered, because of the intrinsic decoupling of extensional and bending behaviour. This is clearly visible by the zero values in K^{T} matrix (16) corresponding to non-zero values in K^{Mod} (17) and K^{Ref} (18) matrices , which are the coupling terms. For this reason, it is considered useful to analyse only K^{Mod} and K^{Ref} matrices for the remaining cases.

$$K^{T} = \begin{bmatrix} 4.3\cdot10^{5} & 0 & 0 & -4.3\cdot10^{5} & 0 & 0 \\ 0 & 2324 & 6197 & 0 & -2324 & 3098 \\ 0 & 6197 & 19191 & 0 & -6197 & 5596 \\ -4.3\cdot10^{5} & 0 & 0 & 4.3\cdot10^{5} & 0 & 0 \\ 0 & -2324 & -6197 & 0 & 2324 & -3098 \\ 0 & 3098 & 5596 & 0 & -3098 & 6798 \end{bmatrix} \quad (16)$$

$$K^{Mod} = \begin{bmatrix} 4.3\cdot10^{5} & 10663 & -385 & -4.3\cdot10^{5} & -10663 & -178 \\ 10663 & 2583 & 6182 & -10663 & -2583 & 3086 \\ -385 & 6182 & 19184 & 385 & -6182 & 5585 \\ -4.3\cdot10^{5} & -10663 & 385 & 4.3\cdot10^{5} & 10663 & 178 \\ -10663 & -2583 & -6182 & 10663 & 2583 & -3086 \\ -178 & 3086 & 5585 & 178 & -3086 & 6777 \end{bmatrix} \quad (17)$$

$$K^{Ref} = \begin{bmatrix} 4.3\cdot10^{5} & 10663 & -356 & -4.3\cdot10^{5} & -10663 & -144 \\ 10686 & 2577 & 6164 & -10663 & -2577 & 3079 \\ -356 & 6164 & 19120 & 356 & -6164 & 5571 \\ -4.3\cdot10^{5} & -10663 & 356 & 4.3\cdot10^{5} & 10663 & 144 \\ -10686 & -2577 & -6164 & 10663 & 2577 & -3079 \\ -144 & 3079 & 5571 & 144 & -3079 & 6755 \end{bmatrix} \quad (18)$$

3.1.2 Estimate of the error

In order to evaluate the size of the error in calculating the stiffness matrices, the following expression is used:

$$(k_{er})_{ij} = \frac{\left| K_{ij}^{Mod} - K_{ij}^{Ref} \right|}{\left| K_{ij}^{Ref} \right|} \quad (19)$$

where K_{ij}^{Mod} is the generic element of the model stiffness matrix and K_{ij}^{Ref} is the corresponding element of the Abaqus stiffness matrix. The $(k_{er})_{ij}$ error is calculated for all elements of the stiffness matrices and for each of the ten analysed case.

The average error of the stiffness matrix related to each single case is evaluated through expression (20), in which e_{rm} is the sum of all $(k_{er})_{ij}$ relating to each relative error matrix:

$$er_{m} = \sum_{i,j=1}^{N} (k_{er})_{ij} \quad (20)$$

In this case, we do not recur to the conventional concept of matrix norms (as example $L1$-*Norm* or $L2$-*Norm*) because with such expressions we neglect the size of the error compared to the entity of the value of each term of the matrix. More simply, adopting expressions (19) and (20) we can take into account the weight of the error of each component of the matrix in the global error.

3.1.3 Results

Figure 4 shows the average error calculated with (20), varying the parameter a from 1 (prismatic section) to 8 (very haunched non-symmetric tapered section), with a constant increasing step of 2. Each case has been evaluated both for slender beam ($L_1 = 4m$) and squat beam ($L_2 = 2m$). After the considerations made at 3.1.1, results based on Timoshenko are reported only for a=2 and L1, showing that solution degrades already in the simplest case.

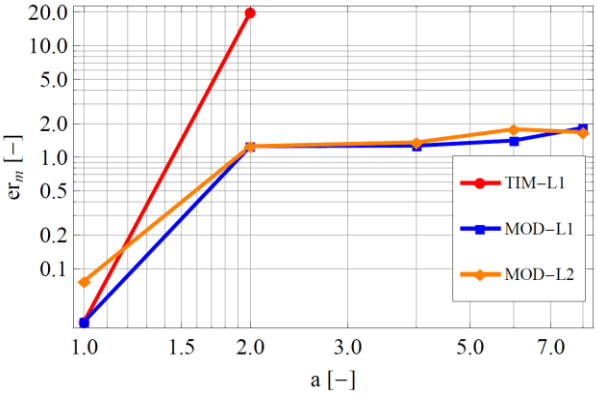

Figure 4: *Non-symmetric tapered beam, Stiffness matrix average error varying the taper ratio a=H/h from 1 to 8, for Timoshenko theory (TIM) and 2D model for H/L1=1/10 and H/L2=1/5 (respectively MOD-L1 and MOD-L2).*

As we can see from Figure 4 the error made with the model for a non-symmetric tapered beam is low and it increases moving from the constant section to the deepest taper section, even if after $a = 2$ the error remains practically constant around the value of 1. It should be notice that the average error comes from the sum of all the 36 relative errors calculated for each component of the matrix, thus an average error of 1 represent a good value. Considering, as example, the error corresponding to $a = 2$ for the MOD-L1 curve, the relative error of each components remains lower than 1%. This is true except for the $(k_{er})_{13}$ and $(k_{er})_{16}$ components which are greater, however, at the same time they represent the less significant terms respect the others comparing the order of magnitude. Referring to Figure 4, the smallest errors related to the beam with length L_1 could be justified by the low value of the slop due to the particular slenderness of the beam. According to the illustrated results, the discrepancies between the reference solution, and model are generally greater in the squat beam case, as expected. It can be noticed that the significant increase of the error appears going from $a = 1$ to $a = 2$, while once the value of 2 is exceeded the trend flattens and the value of average error remains on the same threshold. Consequently, in order to understand the behaviour of the model in that range, we decide to enrich the comparison considering a set of evaluation points between $a = 1$ and $a = 2$. Table 2 summarizes characteristics of the additional 10 cases considered. As in the first part of the parametric study, moving from one case to another, the height H is kept constant and the variable is the lower height h. Figure 5 shows the average error calculated with (20), varying the parameter a from 1 (prismatic section) to 2 (tapered section), with a constant increasing step of 0.25. Each case has been evaluated both for slender beam ($L_1 = 4m$) and squat beam ($L_2 = 2m$).

Table 2: *Summary of studied cases for stiffness matrix evaluation of the non-symmetric tapered case, considering a set of values of the taper ratio* a *between 1 and 2*

L [m]	H [m]	h [m]	a [-]	α [°]
4	0.4	0.4	1	0
4	0.4	0.32	1.25	1.2
4	0.4	0.2666	1.5	1.9
4	0.4	0.2286	1.75	2.5
4	0.4	0.2	2	2.9
2	0.4	0.4	1	0
2	0.4	0.32	1.25	2.3
2	0.4	0.2666	1.5	3.8
2	0.4	0.2286	1.75	4.9
2	0.4	0.2	2	5.7

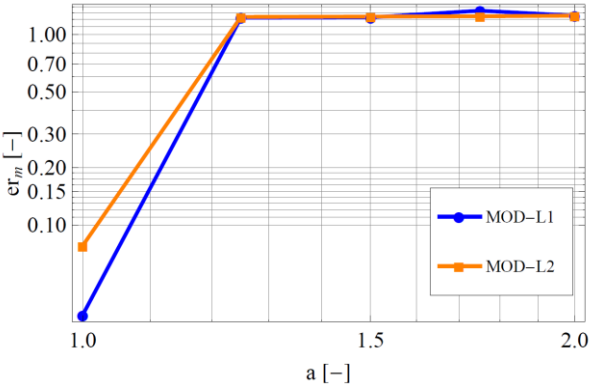

Figure 5: *Non-symmetric tapered beam, Stiffness matrix average error varying the taper ratio a=H/h from 1 to 2 and length L, for 2D model for H/L1=1/10 and H/L2=1/5 (respectively MOD-L1 and MOD-L2).*

The resulting plot from this more accurate evaluation, considering a greater number of point within the interval of interest, confirms what already registered in Figure 4. In fact, results do not seem to be influenced by the taper ratio a after exceeded the value $a=1$ corresponding to the constant cross-section case. Moving towards the tapered geometry, immediately the average error increase and it remains around the value of 1 for all the remaining cases.

3.2 SYMMETRIC TAPERED BEAM: PARAMETRIC STUDY

The second analysed geometry is a symmetric tapered beam in accordance with Figure 3. The parametric study consists in varying the parameter a from 1 to 8 with a constant increasing step of 2, and in considering the ratio $H/L_1=1/10$ (slender beam) and $H/L_2=1/5$ (squat beam). As in the case of non-symmetric tapered geometry, moving from one case to another, the height H is kept constant and the variable is the lower height h. The angles between the lower edge (or the upper edge because of the symmetry) of the beam and the horizontal axis are indicated with α_1 and α_2 respectively for $L_1=4m$ and $L_1=2m$. Table 3 summarizes characteristics of the 10 different cases considered.

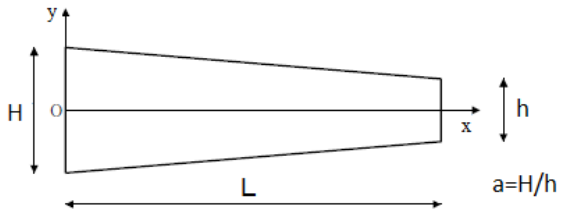

Figure 3: *Symmetric tapered beam geometry*

Table 3: *Summary of studied cases for the stiffness matrix evaluation of the symmetric tapered case*

L1 [m]	H [m]	h [m]	a [-]	α1 [°]
4	0.4	0.4	1	0
4	0.4	0.2	2	1.4
4	0.4	0.1	4	4.3
4	0.4	0.0666	6	4.8
4	0.4	0.05	8	5
2	0.4	0.4	1	0
2	0.4	0.2	2	2.9
2	0.4	0.1	4	8.5
2	0.4	0.0666	6	0.5
2	0.4	0.05	8	10

Concerning results obtained with the FE software Abaqus, we maintain the same modelling hypotheses made for the non-symmetric case. Also considerations on the estimate of the average error remain valid and we adopt for the symmetric case relations (19) and (20) reported in 3.1.2.

3.2.1 Results

Figures 6 shows the average error calculated varying the parameter a from 1 (prismatic section) to 8 (very haunched symmetric tapered section) for slender beam ($L_1=4m$) and squat beam ($L_2=2m$).

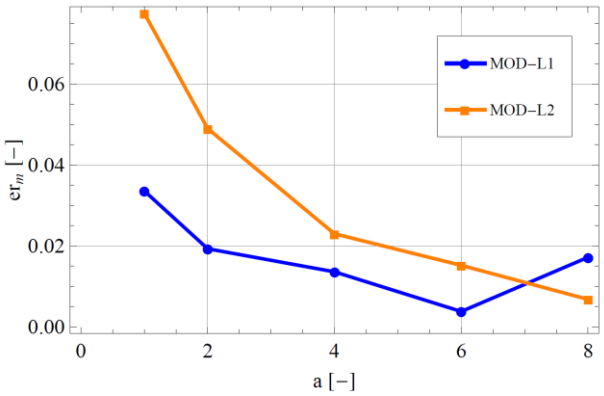

Figure 6: *Symmetric tapered beam, Stiffness matrix average error varying the taper ratio a=H/h and length L, for 2D model for H/L1=1/10 and H/L2=1/5 (respectively MOD-L1 and MOD-L2).*

For the symmetric tapered geometry we register a completely different trend if compared with the non-symmetric one (see Figure 5-6). As we can see from the graph the error made with the model for the symmetric tapered beam is very low and it decreases moving from the constant section to the deepest taper section. These

low values could be explained with the simplification inherent to the symmetric case. Particularly, the symmetric condition leads to have several zero terms in the stiffness matrix (as example the coupling stiffness between the translational and the rotational DOFs). Seeing at Figure 6, the common feature with the non-symmetric tapered case is that even for the symmetric tapered beam discrepancies between FEA and model are generally greater in the squat beam case.

4 CONCLUSIONS

The proposed model represents an efficient and simple tool for the derivation of stiffness matrix of beams with variable cross-section. A comprehensive method for the evaluation of the stiffness matrix for non-prismatic beams has been presented. The developed 2D HR-based model allows to consider any stress and displacement distributions only changing the hypotheses on these field, leading automatically to the final system of ODEs. In this paper, as example, we exploit this potential in order to make possible the use of the well-known relations of prismatic beams (see (12)) also for the case of non-prismatic ones, without interfering with the correctness of the results. To measure the errors made by the model, we conduct numerical analysis using a refined model create in the FE software Abaqus, considered as the reference solution. The results obtained from the comparison between the two approaches shows that model and FE analysis are in good agreement. Furthermore, it can be noticed that even if the variation of the taper ratio parameter and the slenderness of the beam influence the stiffness results, in terms of correctness of matrix evaluation their influence is quite negligible.

Future work will focus on the development of the model to study complex system involving non-prismatic members and to include different constitutive law. Concluding, it could represent a good theoretical model for the developing of a finite element for non-prismatic beams to be integrated in commercial software.

REFERENCES

[1] Boley B.: On the accuracy of the Bernoulli-Euler theory for beams of variable section. Journal of Applied Mechanics, 30(3):373-378, 1963.

[2] El Mezaini N., Balkaya C., Citipitioglu E.: Analysis of frames with nonprismatic members. Journal of Structural Engineering, 117:1573-1592, 1991.

[3] Vu-Quok L., Leger P.: Efficient evaluation of the flexibility of tapered i-beams accounting for shear deformations. International Journal for Numerical Methods in Engineering, 33(3):553-566, 1992.

[4] Hodges D. H., Ho J. C., Yu W.: The effect of taper on section constants for in-plane deformation of an isotropic strip. Journal of Mechanics of Materials and Structures, 3(3):425-440, 2008.

[5] Just D.J.: Plane frameworks of tapering box and i-sections. Journal of the Structural Division, 103(1): 71-86, 1977.

[6] Browns C. J.: Approximate stiffness matrix for tapered beams. Journal of Structural Engineering, 110:3050-3055, 1984.

[7] Eisenberger M.: Explicit stiffness matrix for non-prismatic members. Computer & Structure, 20:715-720, 1984.

[8] Tena Colunga A.: Stiffness formulation for non-prismatic beam elements. Journal of Structural Engineer, 122:1484-1489, 1996.

[9] Balkaya C.: Behavior and modelling of nonprismatic members having T-sections. Journal of Structural Engineering, 127:940-946, 2001.

[10] Zhi-Luo Y. H., Jamali S. M.: Musician S., General form of the stiffness matrix of a tapered beam column. Internation Journal of Mining, Metallurgy & Mechanical Engineering, 1:2320-4060, 2013.

[11] Gimena F., Gonzaga P., Gimena L.: 3d-curved beam element with varying cross-sectional area under generalized. Engineering Structures, 30(2):404-411, 2008.

[12] Gimena F., Gonzaga P., Gimena L.: Structural analysis of a curved beam element defined in global coordinates. Engineering Structures, 30(11):3355-3364, 2008.

[13] Shooshtari A., Khajavi R.: An efficient procedure to find shape functions and stiffness matrices of nonprismatic Euler-Bernoulli and Timoshenko beam elements. European Journal of Mechanics A/Solids , 29:826-836, 2010.

[14] Auricchio F., Balduzzi G., Lovadina C.: A new modeling approach for planar beams: finite-element solutions based on mixed variational derivations. Journal of Mechanics of Materials and Structures, 5(5):771-794, 2010.

[15] Beltempo A., Balduzzi G., Alfano G., Auricchio F.: Analytical derivation of general 2d non-prismatic beam model based on the Hellinger-Reissner principle. Engineering Structures, 101:88-98, 2015.

[16] ABAQUS User's and theory manuals - Release 6.11. Simulia,, Providence, RI, USA, 2011.

[17] Tena Colunga A, Becerril L.A.M.: Lateral stiffness of reinforced concrete moment frames with haunched beams. 15th World Conference on Earthquake Engineering, 2012.